Blood flow analysis in tapered stenosed arteries with influence of heat and mass transfer

Yadong Liu and Wenjun Liu*

College of Mathematics and Statistics, Nanjing University of Information Science and Technology, Nanjing 210044, China

March 19, 2019

Abstract

A non-Newtonian fluid model is used to investigate the two-dimensional pulsatile blood flow through a tapered artery with a stenosis. The mixed convection effects of heat and mass transfer are also taken into account. By applying non-dimensionalization and radial coordinate transformation, we simplify the system in a tube. Under the finite difference scheme, numerical solutions are calculated for velocity, temperature concentration, resistance, impedance, wall shear stress and shearing stress at the stenosis throat. Finally, Quantitative analysis is carried out.

2010 Mathematics Subject Classification: 80A20, 76A05, 76M20.
Keywords: blood flow, stenosed artery, K-L model, heat and mass transfer, finite difference scheme

1 Introduction

The human cardiovascular system is the internal transport of fluids with multiple branches of the arteries in which is a complex blood circulates. The work concerning about bio-fluid dynamical aspects of the human cardiovascular system has gained much attention in recent years with respect to the diagnosis and the genesis of atherosclerosis. Among the various cardiovascular diseases, stenosis is a major one which affects the flow of blood in the arteries. It is associated with pressure distribution, shear stress at the wall and resistance to blood flow. Thus, the study of blood flow through stenosed arteries is important. [9, 17]

Several researchers [25, 27] examined and analyzed the blood flow through a stenosed artery and investigated the effect of physical parameters on blood flow through an arterial stenosis. The effect of tapering on the physiologically important parameters such as wall shear stress, flow rate and resistance to flow has been studied by Bloch [6]. Ku [12], and Kumar [13] discussed the diagnosis and treatment of cardiovascular diseases.

In all the investigations above, blood was treated as Newtonian fluid. However, It has been pointed out that in some diseased conditions, blood exhibits remarkable non-Newtonian properties since it has been seen through experiments that most of the biological fluids exhibit rheology of non-Newtonian characteristics [14, 23]. Therefore, the interest has been non-Newtonian fluid in stenosed artery in recent years.

* Email address: adamliu1127@nuist.edu.cn (Y. D. Liu), wjliu@nuist.edu.cn (W. J. Liu, Corresponding author).

During past decades, numerous investigators focused on different types of fluid in stenosed artery. Nadeem [18] studied blood flow through a tapered artery with a stenosis by Power law fluid model; Chaturani and Samy [8] presented Casson fluid for blood flow through a normal artery with a stenosis by perturbation method; Ali et al. [5] and Zaman et al. [29] captured the rheology of blood by utilizing Sisko fluid model; Ellahi et al. [10] investigated the blood flow as Jeffrey fluid in a catherized tapered artery with the suspension of nanoparticles; Akbar [1–3] modelled blood with Carreau fluid, Walter's B fluid and Sutterby fluid model through a tapered artery with a stenosis, respectively and she also discussed Williamson fluid with pseudoplastic characteristics [4].

At the same time, the system was been more complex under the background of medicine and physic. Mekheimer and El Kot [16] considered blood flow as Sisko fluid and examined the influence of heat and mass transfer; Waqas et al. [26] modeled and analyzed the generalized Burgers fluid subject to Cattaneo-Christov heat flux model; Sankar [20] treated blood as Casson fluid and analyzed the effects of magnetic field through a stenosed artery; Tripathi et al. [24] developed couple stress biofluids with electro-magneto-hydrodynamic properties.

In 1992, Luo and Kuang [14] proposed a new constitutive relation of non-Newtonian fluid which has the property of shear thinning. Motivated by the researches above, we modeled blood as K-L model and investigate the heat and mass transfer of blood flow as no one has studied the K-L model with mixed convection. First, we examine the fluid equation with heat and mass transfer by the constitutive equation of K-L model and choose one geometry of stenosed artery. Then, we use the basic parameters to nondimensionalize the system for further study. Moreover, in order to discrete the system conveniently, we apply the radial coordinate transformation. Finally, we get the numerical solution of velocity, flow rate, resistance and wall shear stress at the stenosis throat by finite difference method.

The paper is arranged as follows. Section 2 gives the formulation of the problem including fluid equations, constitutive equation and geometry of tapered stenosed artery. Section 3 does the nondimensionalization. Section 4 transfers fluid equations by radial coordinate transformation and gives the relation between axial velocity and radial velocity. Section 5 shows the numerical approximation iteration by finite difference method. Section 6 provides the numerical results by graphics.

2 Formulation of the problem

2.1 Geometry of stenosed artery

Consider the flow of blood in an arterial segment treated as a thin, elastic, cylindrical and tapered tube with an axisymmetric overlapping stenosis in its lumen. Let (r, θ, z) be the coordinates of a point in the cylindrical polar coordinates system in which the z-axis is taken along the axis of the artery while r and θ are taken along the radial and the circumferential directions respectively. The geometry of the time-variant overlapping stenosis is constructed mathematically as follows [7]

$$\bar{R}(\bar{z},\bar{t}) = \begin{cases} \Bigg[(m\bar{z}+d_0) - \dfrac{\tau_m \cos(\psi)\left(\bar{z}-\bar{d}\right)}{\bar{l}_0} \\ \qquad \times \left\{ 11 - \dfrac{94\left(\bar{z}-\bar{d}\right)}{3\bar{l}_0} + \dfrac{32\left(\bar{z}-\bar{d}\right)^2}{\bar{l}_0^2} - \dfrac{32\left(\bar{z}-\bar{d}\right)^3}{3\bar{l}_0^3} \right\} \Bigg] \bar{a}_1(\bar{t}), & \bar{d} \le \bar{z} \le \bar{d} + \dfrac{3}{2}\bar{l}_0, \\ (m\bar{z}+d_0)\,\bar{a}_1(\bar{t}), & \text{Otherwise.} \end{cases} \tag{2.1}$$

where $\bar{R}(\bar{z},\bar{t})$ denotes the radius of the artery; $\frac{3\bar{l}_0}{2}$ is the length of overlapping stenosis, ψ is the angle of tapering; $\bar{d}$ is the location of the stenosis; $\bar{L}$ represents the finite length of arterial segment; The slope of the tapered vessel is taken by $m = \tan(\psi)$ and the critical height of the stenosis is given by τ_m. The time-variant parameter $\bar{a}_1(\bar{t})$ is taken to be $\bar{a}_1(\bar{t}) = 1+k_r\cos(\bar{\omega}\bar{t}-\phi)$ where k_r represents the amplitude parameter and ϕ denotes the phase angle. The geometry of stenosed artery is shown in Figure 1.

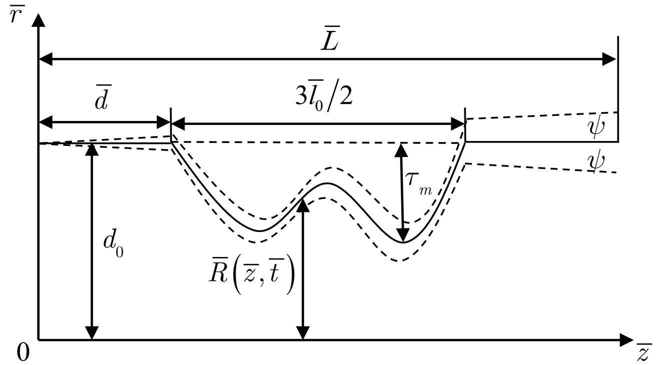

Figure 1: Geometry of the stenosed artery

2.2 Flow equations

Consider the blood flow as incompressible non-Newtonian fluid, we have the continuity equation:

$$\frac{\partial \bar{u}}{\partial \bar{r}} + \frac{\bar{u}}{\bar{r}} + \frac{\partial \bar{w}}{\partial \bar{z}} = 0, \tag{2.2}$$

the momentum equations:

$$\rho\left(\frac{\partial \bar{u}}{\partial \bar{t}} + \bar{u}\frac{\partial \bar{u}}{\partial \bar{r}} + \bar{w}\frac{\partial \bar{u}}{\partial \bar{z}}\right) = -\frac{\partial \bar{p}}{\partial \bar{r}} + \left(\frac{1}{\bar{r}}\frac{\partial}{\partial \bar{r}}\left(\bar{r}\bar{\tau}_{rr}\right) + \frac{\partial}{\partial \bar{r}}\bar{\tau}_{rz}\right), \tag{2.3}$$

$$\begin{aligned}\rho\left(\frac{\partial \bar{w}}{\partial \bar{t}} + \bar{w}\frac{\partial \bar{w}}{\partial \bar{r}} + \bar{w}\frac{\partial \bar{w}}{\partial \bar{z}}\right) = &-\frac{\partial \bar{p}}{\partial \bar{z}} + \left(\frac{1}{\bar{r}}\frac{\partial}{\partial \bar{r}}\left(\bar{r}\bar{\tau}_{rz}\right) + \frac{\partial}{\partial \bar{r}}\bar{\tau}_{zz}\right)\\ &+ \rho\bar{g}\bar{\alpha}\left(\bar{T}-\bar{T}_0\right) + \rho\bar{g}\bar{\alpha}\left(\bar{C}-\bar{C}_0\right),\end{aligned} \tag{2.4}$$

the energy equation:

$$\begin{aligned}\rho c_p\left(\frac{\partial \bar{T}}{\partial \bar{t}} + \bar{u}\frac{\partial \bar{T}}{\partial \bar{r}} + \bar{w}\frac{\partial \bar{T}}{\partial \bar{z}}\right) =&\bar{\tau}_{rr}\frac{\partial \bar{u}}{\partial \bar{r}} + \bar{\tau}_{rz}\frac{\partial \bar{w}}{\partial \bar{r}} + \bar{\tau}_{rz}\frac{\partial \bar{u}}{\partial \bar{z}} + \bar{\tau}_{zz}\frac{\partial \bar{w}}{\partial \bar{z}}\\ &+ k\left(\frac{\partial^2 \bar{T}}{\partial \bar{r}^2} + \frac{1}{r}\frac{\partial \bar{T}}{\partial \bar{r}} + \frac{\partial^2 \bar{T}}{\partial \bar{z}^2}\right),\end{aligned} \tag{2.5}$$

and the mass concentration equation:

$$\begin{aligned}\left(\frac{\partial \bar{C}}{\partial \bar{t}} + \bar{u}\frac{\partial \bar{C}}{\partial \bar{r}} + \bar{w}\frac{\partial \bar{C}}{\partial \bar{z}}\right) =&D\left(\frac{\partial^2 \bar{C}}{\partial \bar{r}^2} + \frac{1}{r}\frac{\partial \bar{C}}{\partial \bar{r}} + \frac{\partial^2 \bar{C}}{\partial \bar{z}^2}\right)\\ &+ \frac{DK_T}{T_m}\left(\frac{\partial^2 \bar{T}}{\partial \bar{r}^2} + \frac{1}{r}\frac{\partial \bar{T}}{\partial \bar{r}} + \frac{\partial^2 \bar{T}}{\partial \bar{z}^2}\right),\end{aligned} \tag{2.6}$$

where ρ is the density of fluid, $\bar{p}$ is the fluid pressure, $\bar{u}$ and $\bar{w}$ are the velocity components in radial and axial directions respectively, $\bar{T}$ is the temperature, $\bar{C}$ is the concentration of fluid, k denotes the thermal conductivity, c_p is the specific heat at constant pressure, T_m

is the temperature of the medium, D is the coefficients of mass diffusivity and K_T is the thermal-diffusion ratio.

The constitutive equation is provided by [14]:

$$\begin{aligned} &\bar{\tau} = \bar{\tau}_0 + \eta_2 \bar{\dot{\gamma}}^{\frac{1}{2}} + \eta_1 \bar{\dot{\gamma}}, \ \bar{\tau} \geq \bar{\tau}_0 \\ &\bar{\dot{\gamma}} = 0, \ \bar{\tau} < \bar{\tau}_0 \end{aligned} \tag{2.7}$$

where $\bar{\tau}_0$, η_1 and η_2 are functions of hematocrit, plasma viscosity and other chemical variable respectively and $\bar{\dot{\gamma}} = \sqrt{\frac{\bar{\Pi}}{2}}$ denotes the shear rate of the fluid, $\bar{\Pi}$ is the second covariant of the system.

Correspondingly, we have

$$\begin{cases} \bar{\tau}_{zz} = 2\bar{\eta}(\bar{\dot{\gamma}}) \left(\dfrac{\partial \bar{w}}{\partial \bar{z}} \right) \\ \bar{\tau}_{rr} = 2\bar{\eta}(\bar{\dot{\gamma}}) \left(\dfrac{\partial \bar{u}}{\partial \bar{r}} \right) \\ \bar{\tau}_{rz} = \bar{\eta}(\bar{\dot{\gamma}}) \left(\dfrac{\partial \bar{w}}{\partial \bar{r}} + \dfrac{\partial \bar{u}}{\partial \bar{z}} \right) \end{cases} \tag{2.8}$$

where $\bar{\eta}(\bar{\dot{\gamma}}) = \frac{\bar{\tau}}{\bar{\dot{\gamma}}}$ represents the apparent viscosity.

The nature of blood flow is pulsatile and the pressure gradient in dimensional form is expressed as [22]

$$-\frac{\partial \bar{p}}{\partial \bar{z}} = \bar{A}_0 + \bar{A}_1 \cos \bar{\omega} \bar{t}, \qquad t > 0.$$

where $\bar{A}_0$ is the amplitude of the steady state pressure gradient, $\bar{A}_1$ is the amplitude of the pulsatile pressure gradient, and the angular frequency $\bar{\omega}$ is expressed as $\bar{\omega} = 2\pi \bar{f}_p$ where $\bar{f}_p$ is the frequency of pulse.

2.3 Initial and Boundary conditions

The initial value for velocity is given by [22],

$$\begin{aligned} \bar{w}(r,z,0) &= \left(\frac{\bar{A}_0 + \bar{A}_1}{4\eta_1} \right) \left[d_0^2 - \left(\frac{\bar{r}}{d_0} \right)^2 \right], \\ \bar{u}(r,z,0) = 0, \ \bar{T}(r,z,0) &= \bar{T}_0, \ \bar{C}(r,z,0) = \bar{C}_0. \end{aligned} \tag{2.9}$$

The boundary conditions are

$$\begin{aligned} \bar{u}(\bar{r},\bar{z},\bar{t}) = 0, \ \frac{\partial \bar{w}}{\partial \bar{r}}(\bar{r},\bar{z},\bar{t}) = 0, \ \frac{\partial \bar{T}}{\partial \bar{r}}(\bar{r},\bar{z},\bar{t}) = 0, \ \frac{\partial \bar{C}}{\partial \bar{r}}(\bar{r},\bar{z},\bar{t}) = 0, \quad \bar{r} = 0, \\ \bar{u}(\bar{r},\bar{z},\bar{t}) = \frac{\partial \bar{R}}{\partial \bar{t}}, \ \bar{w}(\bar{r},\bar{z},\bar{t}) = 0, \ \bar{T}(\bar{r},\bar{z},\bar{t}) = 0, \ \bar{C}(\bar{r},\bar{z},\bar{t}) = 0, \quad \bar{r} = \bar{R}(\bar{z},\bar{t}), \end{aligned} \tag{2.10}$$

3 Non-dimensionalization

Let us introduce non-dimensional quantities as follows:

$$
\begin{aligned}
&r=\frac{\bar{r}}{d_0},\ z=\frac{\bar{z}}{d_0},\ R=\frac{\bar{R}}{d_0},\ u=\frac{\bar{u}}{u_0},\ w=\frac{\bar{w}}{u_0},\ t=\bar{\omega}\bar{t},\ p=\frac{d_0}{u_0\eta_1}\bar{p},\\
&\tau_0=\frac{d_0}{u_0\eta_1}\bar{\tau}_0,\ \tau_{rr}=\frac{d_0}{u_0\eta_1}\bar{\tau}_{rr},\ \tau_{zz}=\frac{d_0}{u_0\eta_1}\bar{\tau}_{zz},\ \tau_{rz}=\frac{d_0}{u_0\eta_1}\bar{\tau}_{rz},\ \alpha^2=\frac{\rho d_0^2\bar{\omega}}{\eta_1},\\
&T=\frac{\bar{T}-\bar{T}_0}{\bar{T}_0},\ C=\frac{\bar{C}-\bar{C}_0}{\bar{C}_0},\ \mathrm{Re}=\frac{\rho d_0 u_0}{\eta_1},\ \mathrm{E_c}=\frac{u_0^2}{c_p\bar{T}_0},\ \mathrm{P_r}=\frac{c_p\eta_1}{k},\ \mathrm{S_r}=\frac{\rho D K_T\bar{T}_0}{\eta_1 T_m\bar{C}_0},\\
&\mathrm{S_c}=\frac{\eta_1}{D\rho},\ \mathrm{G_r}=\frac{g\bar{\alpha}d_0^3\bar{T}_0}{\eta_1^2},\ \mathrm{G_c}=\frac{g\bar{\alpha}d_0^3\bar{C}_0}{\eta_1^2},\ A_0=\frac{d_0^2}{u_0\eta_1}\bar{A}_0,\ A_1=\frac{d_0^2}{u_0\eta_1}\bar{A}_1,
\end{aligned}
\tag{3.1}
$$

where d_0 is the constant radius of the normal artery in the non-stenotic region, u_0 denotes the average velocity of flow in the uniform artery, $\bar{T}_0$ and $\bar{C}_0$ are average temperature and concentration of the fluid respectively. $\mathrm{P_r}$ is the Prandtl number of the fluid, $\mathrm{S_r}$ is Soret number, $\mathrm{E_c}$ is Eckert number, $\mathrm{S_c}$ is Schmidt number, $\mathrm{G_r}$ is Grashof number and $\mathrm{G_c}$ is solutal Grashof number.

As non-dimensional quantities are shown in Eq. (3.1), the dimensionless geometry of stenosed artery is

$$
R(z,t)=\begin{cases}
\left[(mz+d_0)-\dfrac{\tau_m\cos(\psi)(z-d)}{l_0}\right.\\
\qquad\left.\times\left\{11-\dfrac{94(z-d)}{3l_0}+\dfrac{32(z-d)^2}{l_0^2}-\dfrac{32(z-d)^3}{3l_0^3}\right\}\right]a_1(t), & d\le z\le d+\dfrac{3}{2}l_0,\\
(mz+d_0)\,a_1(t), & \text{Otherwise.}
\end{cases}
\tag{3.2}
$$

where $a_1(t)=1+k_r\cos(t-\phi)$.

Similarly, making use of (3.1) along with Eq. (2.2)–(2.6), one obtains that

$$\frac{\partial u}{\partial r}+\frac{u}{r}+\frac{\partial w}{\partial z}=0, \tag{3.3}$$

$$\alpha^2\frac{\partial u}{\partial t}+\mathrm{Re}\left(u\frac{\partial u}{\partial r}+w\frac{\partial u}{\partial z}\right)=-\frac{\partial p}{\partial r}+\left[\frac{\partial}{\partial r}(r\tau_{rr})+\frac{\partial}{\partial z}(\tau_{rz})\right], \tag{3.4}$$

$$\alpha^2\frac{\partial w}{\partial t}+\mathrm{Re}\left(u\frac{\partial w}{\partial r}+w\frac{\partial w}{\partial z}\right)=-\frac{\partial p}{\partial z}+\left[\frac{\partial}{\partial r}(r\tau_{rz})+\frac{\partial}{\partial z}(\tau_{zz})\right]+\mathrm{G_r}T+\mathrm{G_c}C, \tag{3.5}$$

$$
\begin{aligned}
\alpha^2\frac{\partial T}{\partial t}+\mathrm{Re}\left(u\frac{\partial T}{\partial r}+w\frac{\partial T}{\partial z}\right)=&\mathrm{E_c}\left(\tau_{rr}\frac{\partial u}{\partial r}+\tau_{rz}\frac{\partial w}{\partial r}+\tau_{rz}\frac{\partial u}{\partial z}+\tau_{zz}\frac{\partial w}{\partial z}\right)\\
&+\frac{1}{\mathrm{P_r}}\left(\frac{\partial^2 T}{\partial r^2}+\frac{1}{r}\frac{\partial T}{\partial r}+\frac{\partial^2 T}{\partial z^2}\right),
\end{aligned}
\tag{3.6}
$$

$$
\begin{aligned}
\alpha^2\frac{\partial C}{\partial t}+\mathrm{Re}\left(u\frac{\partial C}{\partial r}+w\frac{\partial C}{\partial z}\right)=&\frac{1}{\mathrm{S_c}}\left(\frac{\partial^2 C}{\partial r^2}+\frac{1}{r}\frac{\partial C}{\partial r}+\frac{\partial^2 C}{\partial z^2}\right)\\
&+\mathrm{S_r}\left(\frac{\partial^2 T}{\partial r^2}+\frac{1}{r}\frac{\partial T}{\partial r}+\frac{\partial^2 T}{\partial z^2}\right),
\end{aligned}
\tag{3.7}
$$

in which the dimensionless stress components are

$$\tau_{zz}=2\eta(\dot{\gamma})\left(\frac{\partial w}{\partial z}\right), \tag{3.8}$$

$$\tau_{rr} = 2\eta(\dot\gamma)\left(\frac{\partial u}{\partial r}\right), \tag{3.9}$$

$$\tau_{rz} = \eta(\dot\gamma)\left(\frac{\partial w}{\partial r} + \frac{\partial u}{\partial z}\right), \tag{3.10}$$

$$\eta(\dot\gamma) = \frac{\tau_0 + l\dot\gamma^{\frac{1}{2}} + \dot\gamma}{\dot\gamma}, \quad l = \frac{\eta_2}{\eta_1}\left(\frac{d_0}{u_0}\right)^{\frac{1}{2}}, \tag{3.11}$$

$$\dot\gamma^2 = 2\left[\left(\frac{\partial u}{\partial r}\right)^2 + \left(\frac{u}{r}\right)^2 + \left(\frac{\partial w}{\partial z}\right)^2\right] + \left(\frac{\partial u}{\partial z} + \frac{\partial w}{\partial r}\right)^2. \tag{3.12}$$

Moreover, the dimensionless pressure gradient $-\frac{\partial p}{\partial z}$ appearing in Eq. (3.5) can be written as:

$$-\frac{\partial p}{\partial z} = A_0 + A_1\cos\omega t, \qquad t > 0.$$

Correspondingly, the initial conditions are

$$\begin{gathered} w(r,z,0) = \left(\frac{A_0 + A_1}{4}\right)\left[1 - \left(\frac{r}{d_0}\right)^2\right], \\ u(r,z,0) = 0,\ T(r,z,0) = 0,\ C(r,z,0) = 0. \end{gathered} \tag{3.13}$$

The boundary conditions are

$$\begin{gathered} u(r,z,t) = 0,\ \frac{\partial w}{\partial r}(r,z,t) = 0,\ \frac{\partial T}{\partial r}(r,z,t) = 0,\ \frac{\partial C}{\partial r}(r,z,t) = 0, \quad r = 0, \\ u(r,z,t) = \frac{\partial R}{\partial t},\ w(r,z,t) = 0,\ T(r,z,t) = 0,\ C(r,z,t) = 0, \quad r = R(z,t). \end{gathered} \tag{3.14}$$

4 Radial Coordinate Transformation

In order to fix the vessel wall in the transformed coordinate ξ, we introduce the radial coordinate transformation $\xi = \frac{r}{R(z,t)}$,which was given by [5,7,15]. Under the transformation, Eq. (3.3), (3.5)-(3.7) take the form as follows:

$$\frac{1}{R}\frac{\partial u}{\partial \xi} + \frac{u}{\xi R} + \frac{\partial w}{\partial z} - \frac{\xi}{R}\frac{\partial R}{\partial z}\frac{\partial w}{\partial \xi} = 0, \tag{4.1}$$

$$\begin{aligned} \frac{\partial w}{\partial t} =& \frac{\xi}{R}\frac{\partial R}{\partial t}\frac{\partial w}{\partial \xi} + \frac{\mathrm{Re}}{\alpha^2}\left(-\frac{u}{R}\frac{\partial w}{\partial \xi} + \frac{\xi}{R}\frac{\partial R}{\partial z}w\frac{\partial w}{\partial \xi} - w\frac{\partial w}{\partial \xi}\right) \\ & - \frac{1}{\alpha^2}\frac{\partial p}{\partial z} + \frac{1}{\alpha^2}\left(\frac{1}{\xi R}\tau_{\xi z} + \frac{1}{R}\frac{\partial \tau_{\xi z}}{\partial \xi} - \frac{\partial \tau_{zz}}{\partial z} + \frac{\xi}{R}\frac{\partial R}{\partial z}\frac{\partial \tau_{zz}}{\partial z}\right) + \mathrm{G_r}T + \mathrm{G_c}C, \end{aligned} \tag{4.2}$$

$$\begin{aligned} \frac{\partial T}{\partial t} =& \frac{\xi}{R}\frac{\partial R}{\partial t}\frac{\partial T}{\partial \xi} + \frac{\mathrm{Re}}{\alpha^2}\left(-\frac{u}{R}\frac{\partial T}{\partial \xi} + \frac{\xi}{R}\frac{\partial R}{\partial z}w\frac{\partial T}{\partial \xi} - w\frac{\partial T}{\partial \xi}\right) \\ & + \frac{\mathrm{E_c}}{\alpha^2}\left[\frac{\tau_{\xi\xi}}{R}\frac{\partial u}{\partial \xi} + \frac{\tau_{\xi z}}{R}\frac{\partial w}{\partial \xi} + \tau_{\xi z}\left(\frac{\partial u}{\partial z} - \frac{\xi}{R}\frac{\partial R}{\partial z}\frac{\partial u}{\partial \xi}\right) + \tau_{zz}\left(\frac{\partial w}{\partial z} - \frac{\xi}{R}\frac{\partial R}{\partial z}\frac{\partial w}{\partial \xi}\right)\right] \\ & + \frac{1}{\alpha^2\mathrm{P_r}}\left[\frac{1}{R^2}\frac{\partial^2 T}{\partial \xi^2} + \frac{1}{\xi R^2}\frac{\partial T}{\partial \xi} + \frac{\partial^2 T}{\partial z^2} - \left(-\frac{\xi}{R^2}\frac{\partial R}{\partial z}\frac{\partial T}{\partial \xi} + \frac{\xi}{R}\frac{\partial^2 R}{\partial z^2}\frac{\partial T}{\partial \xi} + \frac{\xi}{R}\frac{\partial R}{\partial z}\frac{\partial^2 T}{\partial \xi^2}\right)\right], \end{aligned} \tag{4.3}$$

$$
\begin{aligned}
\frac{\partial C}{\partial t} =& \frac{\xi}{R}\frac{\partial R}{\partial t}\frac{\partial C}{\partial \xi} + \frac{\mathrm{Re}}{\alpha^2}\left(-\frac{u}{R}\frac{\partial C}{\partial \xi} + \frac{\xi}{R}\frac{\partial R}{\partial z}w\frac{\partial C}{\partial \xi} - w\frac{\partial C}{\partial \xi}\right) \\
&+ \frac{\mathrm{S_r}}{\alpha^2}\left[\frac{1}{R^2}\frac{\partial^2 T}{\partial \xi^2} + \frac{1}{\xi R^2}\frac{\partial T}{\partial \xi} + \frac{\partial^2 T}{\partial z^2} - \left(-\frac{\xi}{R^2}\frac{\partial R}{\partial z}\frac{\partial T}{\partial \xi} + \frac{\xi}{R}\frac{\partial^2 R}{\partial z^2}\frac{\partial T}{\partial \xi} + \frac{\xi}{R}\frac{\partial R}{\partial z}\frac{\partial^2 T}{\partial \xi^2}\right)\right] \\
&+ \frac{1}{\alpha^2 \mathrm{S_c}}\left[\frac{1}{R^2}\frac{\partial^2 C}{\partial \xi^2} + \frac{1}{\xi R^2}\frac{\partial C}{\partial \xi} + \frac{\partial^2 C}{\partial z^2} - \left(-\frac{\xi}{R^2}\frac{\partial R}{\partial z}\frac{\partial C}{\partial \xi} + \frac{\xi}{R}\frac{\partial^2 R}{\partial z^2}\frac{\partial C}{\partial \xi} + \frac{\xi}{R}\frac{\partial R}{\partial z}\frac{\partial^2 C}{\partial \xi^2}\right)\right],
\end{aligned}
\tag{4.4}
$$

where stress components are

$$
\tau_{zz} = 2\eta(\dot{\gamma})\left(\frac{\partial w}{\partial z} - \frac{\xi}{R}\frac{\partial R}{\partial z}\frac{\partial w}{\partial \xi}\right), \tag{4.5}
$$

$$
\tau_{\xi\xi} = 2\eta(\dot{\gamma})\left(\frac{1}{R}\frac{\partial u}{\partial \xi}\right), \tag{4.6}
$$

$$
\tau_{\xi z} = \eta(\dot{\gamma})\left(\frac{\partial u}{\partial z} - \frac{\xi}{R}\frac{\partial R}{\partial z}\frac{\partial u}{\partial \xi} + \frac{1}{R}\frac{\partial w}{\partial \xi}\right), \tag{4.7}
$$

$$
\eta(\dot{\gamma}) = \frac{\tau_0 + l\dot{\gamma}^{\frac{1}{2}} + \dot{\gamma}}{\dot{\gamma}}, \quad l = \frac{\eta_2}{\eta_1}\left(\frac{d_0}{u_0}\right)^{\frac{1}{2}}, \tag{4.8}
$$

$$
\begin{aligned}
\dot{\gamma}^2 =& 2\left[\left(\frac{\partial u}{\partial \xi}\frac{1}{R}\right)^2 + \left(\frac{u}{\xi R}\right)^2 + \left(\frac{\partial w}{\partial z} - \frac{\xi}{R}\frac{\partial R}{\partial z}\frac{\partial w}{\partial \xi}\right)^2\right] \\
&+ \left(\frac{\partial u}{\partial z} - \frac{\xi}{R}\frac{\partial R}{\partial z}\frac{\partial u}{\partial \xi} + \frac{1}{R}\frac{\partial w}{\partial \xi}\right)^2.
\end{aligned}
\tag{4.9}
$$

Multiplying Eq. (4.1) by ξR and integrating with respect to ξ from 0 to ξ, we get

$$
u(\xi, z, t) = \xi\frac{\partial R}{\partial \xi}w - \frac{R}{\xi}\int_0^{\xi}\xi\frac{\partial w}{\partial z}d\xi - \frac{2}{\xi}\int_0^{\xi}\xi w d\xi, \tag{4.10}
$$

for $\xi = 1$, using the boundary conditions. (4.10) becomes

$$
-\int_0^1 \xi\frac{\partial w}{\partial \xi}d\xi = \int_0^1 \xi\left[\frac{2}{R}\frac{\partial R}{\partial z}w + \frac{1}{R}\frac{\partial R}{\partial t}f(\xi)\right]d\xi, \tag{4.11}
$$

where $f(\xi)$ represents an arbitrary function satisfying $\int_0^1 \xi f(\xi)d\xi = 1$. Therefore, we chose $f(\xi)$ as $f(\xi) = 4\left(\xi^2 - 1\right)$. Taking the approximation of the equality between the integrals to integrands from (4.11), we have

$$
\frac{\partial w}{\partial z} = -\frac{2}{R}\frac{\partial R}{\partial z}w + \frac{4}{R}\left(\xi^2 - 1\right)\frac{\partial R}{\partial t}, \tag{4.12}
$$

substituting (4.12) into (4.10), we finally arrive at

$$
u(\xi, z, t) = \xi\left[\frac{\partial R}{\partial z}w + \frac{\partial R}{\partial t}\left(2 - \xi^2\right)\right]. \tag{4.13}
$$

Conditions (3.13) and (3.14) can be written as

$$
w(\xi, z, 0) = \left(\frac{A_0 + A_1}{4}\right)\left[1 - \left(\frac{\xi R}{d_0}\right)^2\right],
$$

$$
u(\xi, z, 0) = 0,\ T(\xi, z, 0) = 0,\ C(\xi, z, 0) = 0.
$$

$$
u(\xi, z, t) = 0,\ \frac{\partial w}{\partial \xi}(\xi, z, t) = 0,\ \frac{\partial T}{\partial \xi}(\xi, z, t) = 0,\ \frac{\partial C}{\partial \xi}(\xi, z, t) = 0, \quad r = 0,
$$

$$
u(\xi, z, t) = \frac{\partial R}{\partial t},\ w(\xi, z, t) = 0,\ T(\xi, z, t) = 0,\ C(\xi, z, t) = 0, \quad r = R(z, t),
$$

5 Numerical Approximation

In this section, we apply the finite difference method to solve the problem. specifically, central difference scheme is carried out in spatial dimension while forward difference scheme is adapted in time dimension as in following manner(Difference of u, T, C and relevant derivatives can also be obtained by similar expression):

$$(w_\xi)_{i,j}^k = \frac{\partial w}{\partial \xi} = \frac{(w)_{i,j+1}^k - (w)_{i,j-1}^k}{2\Delta\xi}, \tag{5.1}$$

$$(w_z)_{i,j}^k = \frac{\partial w}{\partial z} = \frac{(w)_{i+1,j}^k - (w)_{i-1,j}^k}{2\Delta z}, \tag{5.2}$$

$$\frac{\partial w}{\partial t} = \frac{(w)_{i,j}^{k+1} - (w)_{i,j}^k}{\Delta t}, \tag{5.3}$$

$$(w_{\xi\xi})_{i,j}^k = \frac{\partial^2 w}{\partial \xi^2} = \frac{(w)_{i,j+1}^k - (w)_{i,j}^k + (w)_{i,j-1}^k}{(\Delta\xi)^2}, \tag{5.4}$$

$$(w_{zz})_{i,j}^k = \frac{\partial^2 w}{\partial z^2} = \frac{(w)_{i+1,j}^k - (w)_{i,j}^k + (w)_{i-1,j}^k}{(\Delta z)^2}, \tag{5.5}$$

$$(w_{\xi z})_{i,j}^k = \frac{\partial^2 w}{\partial \xi \partial z} = \frac{(w)_{i+1,j+1}^k - (w)_{i-1,j+1}^k - (w)_{i+1,j-1}^k + (w)_{i-1,j-1}^k}{4\Delta\xi\Delta z}, \tag{5.6}$$

$$\tag{5.7}$$

where

$$\begin{cases} \xi_j = (j-1)\,\Delta\xi, & (j = 1, 2, ..., N+1)\,,\ \xi_{N+1} = 1, \\ z_i = (i-1)\,\Delta z, & (i = 1, 2, ..., M+1)\,, \\ t_k = (k-1)\,\Delta t, & (k = 1, 2, ...)\,. \end{cases}$$

Then we can deduced difference form as follows according to Eq. (4.5)-(4.9).

$$\begin{aligned} \left((\dot\gamma)_{i,j}^k\right)^2 =& 2\left[\left(\frac{(u_\xi)_{i,j}^k}{R_i^k}\right)^2 + \left(\frac{u_{i,j}^k}{\xi_j R_i^k}\right)^2 + \left((w_z)_{i,j}^k - \frac{\xi_j\,(R_z)_i^k\,(w_\xi)_{i,j}^k}{R_i^k}\right)^2\right] \\ &+ \left((u_z)_{i,j}^k - \frac{\xi_j\,(R_z)_i^k\,(u_\xi)_{i,j}^k}{R_i^k} + \frac{(w_\xi)_{i,j}^k}{R_i^k}\right)^2, \end{aligned} \tag{5.8}$$

$$\begin{aligned} (\dot\gamma_\xi)_{i,j}^k = \frac{\partial \dot\gamma}{\partial \xi} = \frac{1}{\dot\gamma_{i,j}^k} &\left[2\frac{(u_\xi)_{i,j}^k\,(u_{\xi\xi})_{i,j}^k}{\left(R_i^k\right)^2} + 2\frac{u_{i,j}^k\left(\xi_j\,(u_\xi)_{i,j}^k - u_{i,j}^k\right)}{(\xi_j)^3\left(R_i^k\right)^2} + 2\left((w_z)_{i,j}^k - \frac{\xi_j\,(R_z)_i^k\,(w_\xi)_{i,j}^k}{R_i^k}\right)\right. \\ &\times \left.\left((w_{\xi z})_{i,j}^k - \frac{(R_z)_i^k\,(w_\xi)_{i,j}^k + \xi_j\,(w_{\xi\xi})_{i,j}^k}{R_i^k}\right)\right] + \frac{1}{\dot\gamma_{i,j}^k}\left((u_z)_{i,j}^k + \frac{(w_\xi)_{i,j}^k - (R_z)_i^k\,(u_\xi)_{i,j}^k}{R_i^k}\right) \\ &\times \left((u_{\xi z})_{i,j}^k + \frac{(w_{\xi\xi})_{i,j}^k - (R_z)_i^k\left((u_\xi)_{i,j}^k + \xi_j\,(u_{\xi z})_{i,j}^k\right)}{R_i^k}\right), \end{aligned} \tag{5.9}$$

$$
\begin{aligned}
(\dot{\gamma}_z)_{i,j}^k = \frac{\partial \dot{\gamma}}{\partial z} = \frac{1}{\dot{\gamma}_{i,j}^k} \Bigg[& 2\frac{(u_\xi)_{i,j}^k \left(R_i^k (u_{\xi z})_{i,j}^k - (R_z)_i^k (u_\xi)_{i,j}^k\right)}{\left(R_i^k\right)^3} + 2\frac{u_{i,j}^k \left(R_i^j (u_z)_{i,j}^k - (R_z)_i^k u_{i,j}^k\right)}{(\xi_j)^2 \left(R_i^k\right)^3} \\
& +2\left((w_z)_{i,j}^k - \frac{\xi_j (R_z)_i^k (w_\xi)_{i,j}^k}{R_i^k}\right) \Bigg((w_{zz})_{i,j}^k + \xi_j \frac{\left((R_z)_i^k\right)^2 (w_\xi)_{i,j}^k}{\left(R_i^k\right)^2} \\
& +\xi_j \frac{(R_{zz})_i^k (w_\xi)_{i,j}^k + (R_z)_i^k (w_{\xi z})_{i,j}^k}{R_i^k} \Bigg) \Bigg] + \frac{1}{\dot{\gamma}_{i,j}^k} \left((u_z)_{i,j}^k + \frac{(w_\xi)_{i,j}^k - (R_z)_i^k (u_\xi)_{i,j}^k}{R_i^k} \right) \\
& \times \Bigg((u_{zz})_{i,j}^k + \xi_j \frac{(R_{zz})_i^k (u_\xi)_{i,j}^k + (R_z)_i^k (u_{\xi z})_{i,j}^k}{R_i^k} \\
& + \frac{\xi_j \left((R_z)_i^k\right)^2 (u_\xi)_{i,j}^k + R_i^k (w_{\xi z})_{i,j}^k - (R_z)_i^k (w_\xi)_{i,j}^k}{\left(R_i^k\right)^2} \Bigg),
\end{aligned}
\tag{5.10}
$$

$$
(\eta(\dot{\gamma}))_{i,j}^k = \frac{\tau_0 + l\left((\dot{\gamma})_{i,j}^k\right)^{\frac{1}{2}} + (\dot{\gamma})_{i,j}^k}{(\dot{\gamma})_{i,j}^k} = \tau_0 \left((\dot{\gamma})_{i,j}^k\right)^{-1} + l\left((\dot{\gamma})_{i,j}^k\right)^{-\frac{1}{2}}, \tag{5.11}
$$

$$
(\eta_\xi(\dot{\gamma}))_{i,j}^k = \frac{\partial \eta(\dot{\gamma})}{\partial \xi} = \left(-\tau_0 \left((\dot{\gamma})_{i,j}^k\right)^{-2} - \frac{l}{2}\left((\dot{\gamma})_{i,j}^k\right)^{-\frac{3}{2}}\right) (\dot{\gamma}_\xi)_{i,j}^k, \tag{5.12}
$$

$$
(\eta_z(\dot{\gamma}))_{i,j}^k = \frac{\partial \eta(\dot{\gamma})}{\partial z} = \left(-\tau_0 \left((\dot{\gamma})_{i,j}^k\right)^{-2} - \frac{l}{2}\left((\dot{\gamma})_{i,j}^k\right)^{-\frac{3}{2}}\right) (\dot{\gamma}_z)_{i,j}^k. \tag{5.13}
$$

What's more, Eq. (4.5)–(4.7) give that

$$
(\tau_{zz})_{i,j}^k = 2\eta_{i,j}^k \left(w_z - \frac{\xi_j (R_z)_i^k (w_\xi)_{i,j}^k}{R_i^k} \right), \tag{5.14}
$$

$$
(\tau_{\xi\xi})_{i,j}^k = 2\eta_{i,j}^k \left(\frac{(u_\xi)_{i,j}^k}{R_i^k} \right), \tag{5.15}
$$

$$
(\tau_{\xi z})_{i,j}^k = \eta_{i,j}^k \left(u_z - \frac{\xi_j (R_z)_i^k (u_\xi)_{i,j}^k}{R_i^k} + \frac{(w_\xi)_{i,j}^k}{R_i^k} \right), \tag{5.16}
$$

and the difference form of corresponding partial derivatives:

$$
\begin{aligned}
\left[(\tau_{zz})_\xi\right]_{i,j}^k = \frac{\partial \tau_{zz}}{\partial \xi} =& 2(\eta_\xi)_{i,j}^k \left((w_z)_{i,j}^k - \frac{\xi_j (R_z)_i^k (w_\xi)_{i,j}^k}{R_i^k} \right) \\
& + 2\eta_{i,j}^k \left((w_{\xi z})_{i,j}^k - \frac{(R_z)_i^k \left((w_\xi)_{i,j}^k + \xi_j (w_{\xi\xi})_{i,j}^k\right)}{R_i^k} \right),
\end{aligned}
\tag{5.17}
$$

$$
\begin{aligned}
\left[(\tau_{zz})_z\right]_{i,j}^k = \frac{\partial \tau_{zz}}{\partial z} =& 2(\eta_z)_{i,j}^k \left((w_z)_{i,j}^k - \frac{\xi_j (R_z)_i^k (w_\xi)_{i,j}^k}{R_i^k} \right) + 2\eta_{i,j}^k \Bigg((w_{zz})_{i,j}^k \\
& + \xi_j \frac{\left((R_z)_i^k\right)^2 (w_\xi)_{i,j}^k}{\left(R_i^k\right)^2} + \xi_j \frac{(R_{zz})_i^k (w_\xi)_{i,j}^k + (R_z)_i^k (w_{\xi z})_{i,j}^k}{R_i^k} \Bigg),
\end{aligned}
\tag{5.18}
$$

$$\left[(\tau_{\xi z})_{\xi}\right]_{i,j}^{k} = \frac{\partial \tau_{\xi z}}{\partial \xi} = (\eta_{\xi})_{i,j}^{k}\left((u_z)_{i,j}^{k} + \frac{(w_{\xi})_{i,j}^{k} - (R_z)_i^k (u_{\xi})_{i,j}^{k}}{R_i^k}\right)$$
$$+ \eta_{i,j}^{k}\left((u_{\xi z})_{i,j}^{k} + \frac{(w_{\xi\xi})_{i,j}^{k} - (R_z)_i^k \left((u_{\xi})_{i,j}^{k} + \xi_j (u_{\xi z})_{i,j}^{k}\right)}{R_i^k}\right), \tag{5.19}$$

$$\left[(\tau_{\xi z})_{z}\right]_{i,j}^{k} = \frac{\partial \tau_{\xi z}}{\partial z} = (\eta_{z})_{i,j}^{k}\left((u_z)_{i,j}^{k} + \frac{(w_{\xi})_{i,j}^{k} - (R_z)_i^k (u_{\xi})_{i,j}^{k}}{R_i^k}\right) + \eta_{i,j}^{k}\left((u_{zz})_{i,j}^{k}\right.$$
$$+\frac{\xi_j \left((R_z)_i^k\right)^2 (u_{\xi})_{i,j}^{k} + R_i^k (w_{\xi z})_{i,j}^{k} - (R_z)_i^k (w_{\xi})_{i,j}^{k}}{\left(R_i^k\right)^2} \tag{5.20}$$
$$\left.+\xi_j \frac{(R_{zz})_i^k (u_{\xi})_{i,j}^{k} + (R_z)_i^k (u_{\xi z})_{i,j}^{k}}{R_i^k}\right).$$

With Eq. (5.1)–(5.20), the iteration formulas of the fluid can be deduced from Eq. (4.2)–(4.4) that

$$w_{i,j}^{k+1} = w_{i,j}^{k} + \Delta t \left\{ \frac{\xi_j}{R_i^k} (R_t)_i^k (w_{\xi})_{i,j}^{k} \right.$$
$$+\frac{\mathrm{Re}}{\alpha^2}\left[-\frac{u_{i,j}^{k}}{R_i^k}(w_{\xi})_{i,j}^{k} + \frac{\xi_j}{R_i^k}(R_z)_i^k w_{i,j}^{k} (w_{\xi})_{i,j}^{k} - w_{i,j}^{k} (w_z)_{i,j}^{k}\right]$$
$$-\frac{1}{\alpha^2}\left(\frac{\partial p}{\partial z}\right)^k + \frac{1}{\alpha^2}\left[\frac{(\tau_{\xi z})_{i,j}^{k}}{\xi_j R_i^k} + \frac{\left[(\tau_{\xi z})_{\xi}\right]_{i,j}^{k}}{R_i^k} - \left[(\tau_{zz})_z\right]_{i,j}^{k}\right. \tag{5.21}$$
$$\left.\left.+\frac{\xi_j (R_z)_i^k \left[(\tau_{zz})_{\xi}\right]_{i,j}^{k}}{R_i^k}\right] + \mathrm{G_r} T_{i,j}^{k} + \mathrm{G_c} C_{i,j}^{k}\right\},$$

$$u_{i,j}^{k+1} = \xi_j \left[(R_z)_i^{k+1} w_{i,j}^{k+1} + (R_t)_i^{k+1}\left(2 - (\xi_j)^2\right)\right], \tag{5.22}$$

$$T_{i,j}^{k+1} = T_{i,j}^{k} + \Delta t \left\{ \frac{\xi_j}{R_i^k} (R_t)_i^k (T_{\xi})_{i,j}^{k} \right.$$
$$+\frac{\mathrm{Re}}{\alpha^2}\left[-\frac{u_{i,j}^{k}}{R_i^k}(T_{\xi})_{i,j}^{k} + \frac{\xi_j}{R_i^k}(R_z)_i^k w_{i,j}^{k} (T_{\xi})_{i,j}^{k} - w_{i,j}^{k} (T_z)_{i,j}^{k}\right]$$
$$+\frac{\mathrm{E_c}}{\alpha^2}\left[(\tau_{\xi z})_{i,j}^{k} (u_z)_{i,j}^{k} + (\tau_{zz})_{i,j}^{k} (w_z)_{i,j}^{k} + \frac{(\tau_{\xi\xi})_{i,j}^{k} (u_{\xi})_{i,j}^{k} + (\tau_{\xi z})_{i,j}^{k} (w_{\xi})_{i,j}^{k}}{R_i^k}\right.$$
$$\left.-\frac{(\tau_{\xi z})_{i,j}^{k} \xi_j (R_z)_i^k (u_{\xi})_{i,j}^{k} + (\tau_{zz})_{i,j}^{k} \xi_j (R_z)_i^k (w_{\xi})_{i,j}^{k}}{R_i^k}\right] \tag{5.23}$$
$$+\frac{1}{\alpha^2 \mathrm{P_r}}\left[\frac{(T_{\xi\xi})_{i,j}^{k}}{\left(R_i^k\right)^2} + \frac{(T_{\xi})_{i,j}^{k}}{\xi_j \left(R_i^k\right)^2} + (T_{zz})_{i,j}^{k}\right.$$
$$\left.\left.+\frac{\xi_j (R_z)_i^k (T_{\xi})_{i,j}^{k}}{\left(R_i^k\right)^2} - \frac{\xi_j (R_{zz})_i^k (T_{\xi})_{i,j}^{k}}{R_i^k} - \frac{\xi_j (R_z)_i^k (T_{\xi z})_{i,j}^{k}}{R_i^k}\right]\right\},$$

$$
\begin{aligned}
C_{i,j}^{k+1} = C_{i,j}^{k} + \Delta t \Bigg\{ & \frac{\xi_j}{R_i^k} \left(R_t\right)_i^k \left(C_\xi\right)_{i,j}^k \\
& + \frac{\mathrm{Re}}{\alpha^2} \left[-\frac{u_{i,j}^k}{R_i^k} \left(C_\xi\right)_{i,j}^k + \frac{\xi_j}{R_i^k} \left(R_z\right)_i^k w_{i,j}^k \left(C_\xi\right)_{i,j}^k - w_{i,j}^k \left(C_z\right)_{i,j}^k \right] \\
& + \frac{\mathrm{S_r}}{\alpha^2} \left[\frac{\left(T_{\xi\xi}\right)_{i,j}^k}{\left(R_i^k\right)^2} + \frac{\left(T_\xi\right)_{i,j}^k}{\xi_j \left(R_i^k\right)^2} + \left(T_{zz}\right)_{i,j}^k \right. \\
& \left. + \frac{\xi_j \left(R_z\right)_i^k \left(T_\xi\right)_{i,j}^k}{\left(R_i^k\right)^2} - \frac{\xi_j \left(R_{zz}\right)_i^k \left(T_\xi\right)_{i,j}^k}{R_i^k} - \frac{\xi_j \left(R_z\right)_i^k \left(T_{\xi z}\right)_{i,j}^k}{R_i^k} \right] \\
& + \frac{1}{\alpha^2 \mathrm{S_c}} \left[\frac{\left(C_{\xi\xi}\right)_{i,j}^k}{\left(R_i^k\right)^2} + \frac{\left(C_\xi\right)_{i,j}^k}{\xi_j \left(R_i^k\right)^2} + \left(C_{zz}\right)_{i,j}^k \right. \\
& \left. + \frac{\xi_j \left(R_z\right)_i^k \left(C_\xi\right)_{i,j}^k}{\left(R_i^k\right)^2} - \frac{\xi_j \left(R_{zz}\right)_i^k \left(C_\xi\right)_{i,j}^k}{R_i^k} - \frac{\xi_j \left(R_z\right)_i^k \left(C_{\xi z}\right)_{i,j}^k}{R_i^k} \right] \Bigg\},
\end{aligned}
\tag{5.24}
$$

and corresponding initial and boundary conditions are

$$
\begin{gathered}
w_{i,j}^1 = \left(\frac{A_0 + A_1}{4} \right) \left[1 - \left(\frac{\xi_j R_i^1}{d_0} \right)^2 \right], \\
u_{i,j}^1 = 0, \quad T_{i,j}^1 = 1, \quad C_{i,j}^1 = 1, \\
w_{i,1}^k = u_{i,1}^k = 0, \quad w_{i,1}^k = w_{i,2}^k, \quad w_{i,N+1}^k = 0, \quad u_{i,N+1}^k = \left(\frac{\partial R}{\partial t} \right)_i^k .
\end{gathered}
$$

The volumetric flow rate (Q), the resistance impedance (Λ) and the wall shear stress (τ_w) are given by [15]

$$
Q_i^k = 2\pi \left(R_i^k \right)^2 \int_0^1 \xi_j w_{i,j}^k d\xi_j, \tag{5.25}
$$

$$
\Lambda_i^k = \frac{\left| L \left(\frac{\partial p}{\partial z} \right)^k \right|}{Q_i^k}, \tag{5.26}
$$

$$
\left(\tau_w\right)_i^k = \left(\tau_{\xi z}\right)_{i,N+1}^k . \tag{5.27}
$$

6 Results and Discussion

In this section, graphical results are displayed and The quantitative effects of parameters are discussed. As in [8, 11], we have parameters that

$$
\begin{gathered}
d_0 = 1,\ A_0 = 1,\ A_1 = 0.2A_0,\ \phi = 0,\ k_r = 0.05 \\
f_p = 1.2,\ L_0 = 15,\ d = 7,\ L = 30.
\end{gathered}
$$

We take $\Delta\xi = 0.1$ and $\Delta z = 0.1$ along the radial direction and axial direction respectively and time step $\Delta t = 0.001$ which assures the convergence of the numerical solution. The numerical solutions for velocity, flow rate, shear stress, resistive impedance, temperature, and concentration distributions for various values of parameters involved in the present study are computed numerically using MATLAB programming.

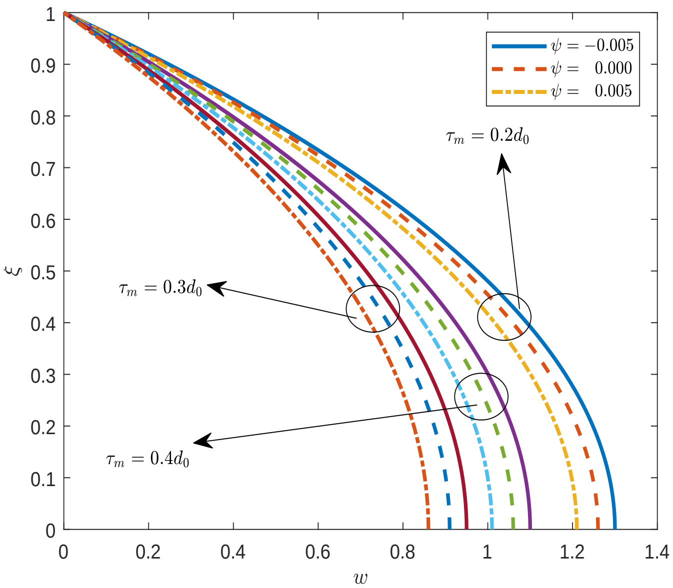

Figure 2: Variation of axial velocity for $z = 10, t = 0.2, \mathrm{Re} = 1000, \alpha^2 = 2000, \tau_0 = 1, l = 4, \mathrm{E_c} = 0.4, \mathrm{P_r} = 3, \mathrm{S_r} = 3, \mathrm{S_c} = 3, \mathrm{G_r} = 1.5, \mathrm{G_c} = 1.5$.

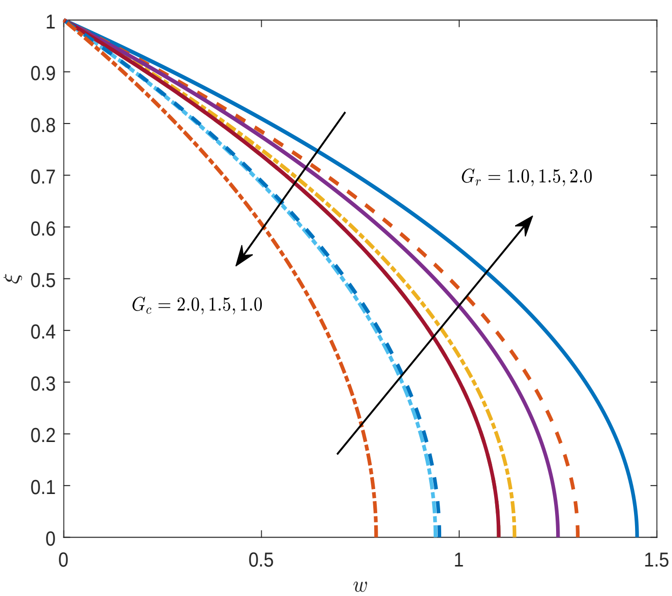

Figure 3: Variation of axial velocity for $z = 10, t = 0.2, \tau_m = 0.3d_0, \mathrm{Re} = 1000, \alpha^2 = 2000, \tau_0 = 1, l = 4, \mathrm{E_c} = 0.4, \mathrm{P_r} = 3, \mathrm{S_r} = 3, \mathrm{S_c} = 3$.

6.1 Velocity distribution

Figure 2 shows the velocity distribution for different values of ψ and τ_m with $z = 10, t = 0.2, \mathrm{Re} = 1000, \alpha^2 = 2000, \tau_0 = 1, l = 4, \mathrm{E_c} = 0.4, \mathrm{P_r} = 3, \mathrm{S_r} = 3, \mathrm{S_c} = 3, \mathrm{G_r} = 1.5, \mathrm{G_c} = 1$. Under the assumption that the blood vessel is axial symmetric, it is obviously that blood flow velocity reaches the maximum value at the center of the artery from Figure 2. With the increase of maximum depth of the stenosis τ_m, the velocity of blood decreases considerably while it will also decrease as the angle of tapered vessel increases. We can also conclude that the velocity varies like a parabolic function at ξ. Thus, reducing the stenosis in the blood vessel is important to accelerate the blood velocity.

Fixing the critical height of stenosis at $\tau_m = 0.3d_0$ and varying $\mathrm{G_r}$ and $\mathrm{G_c}$, we have different velocity profile with different $\mathrm{G_r}$ and $\mathrm{G_c}$ on Figure 3. Thus, we can obtain that the velocity increase with the rise of Grashof number $\mathrm{G_r}$ and solutal Grashof number $\mathrm{G_c}$ which represent the heat effects and mass effect on fluid respectively. That means with the growth of temperature and concentration, the velocity will increase a lot correspondingly.

6.2 Flow rate

Figure 4 illustrates the profiles for volumetric flow rate in stenosed artery for three different taper angles and G_r with $t = 0.2, \tau_m = 0.3d_0, \mathrm{Re} = 1000, \alpha^2 = 2000, \tau_0 = 1, l = 4, \mathrm{E_c} = 0.3, \mathrm{P_r} = 3, \mathrm{S_r} = 3, \mathrm{S_c} = 3, \mathrm{G_c} = 1.5$. It is seen that the volumetric flow rate distribution is shaped like the geometry of the stenosis, which is that at the beginning of the stenosis the flow rate dropped and at the stenosis critical height, it reaches to its Minimum. What's more, With the increase of the taper angle, the flow rate grows up considerably. It can also be obtained in Figure 4 that as thermodynamics parameter Grashof number $\mathrm{G_r}$ increases, the flow rate grows up.

Figure 5 shows that under the effect of the mass transfer in fluid which can be illustrated by solutal Grashof number $\mathrm{G_c}$, the flow rate will have a different increases as $\mathrm{G_c}$ increases. The positive feedback can guide people to take effective action to enhance the flow rate.

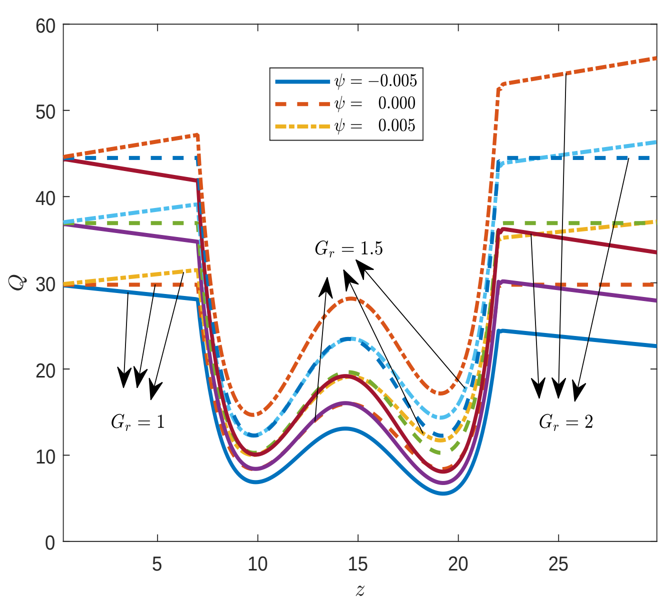

Figure 4: Variation of flow rate for $t = 0.2, \tau_m = 0.3d_0, \mathrm{Re} = 1000, \alpha^2 = 2000, \tau_0 = 1, l = 4, \mathrm{E_c} = 0.4, \mathrm{P_r} = 3, \mathrm{S_r} = 3, \mathrm{S_c} = 3, \mathrm{G_c} = 1.5$.

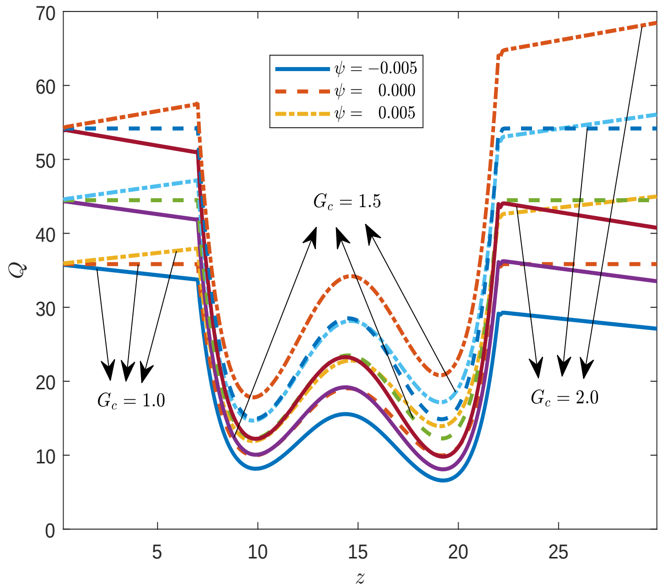

Figure 5: Variation of flow rate for $t = 0.2, \tau_m = 0.3d_0, \mathrm{Re} = 1000, \alpha^2 = 2000, \tau_0 = 1, l = 4, \mathrm{E_c} = 0.4, \mathrm{P_r} = 3, \mathrm{S_r} = 3, \mathrm{S_c} = 3, \mathrm{G_c} = 1.5$.

6.3 Wall shear stress

Figure 6 and Figure 7 are prepared to observe the variation of the shear stress at stenosis for different tapered angle with Grashof number $\mathrm{G_r}$ and solutal Grashof number $\mathrm{G_c}$ with $t = 0.2, \tau_m = 0.3d_0, \mathrm{Re} = 1000, \alpha^2 = 2000, \tau_0 = 1, l = 4, \mathrm{E_c} = 0.3, \mathrm{P_r} = 3, \mathrm{S_r} = 3, \mathrm{S_c} = 3$. It is observed that the wall shear stress yields diverging tapering with tapered angle $\psi > 0$, converging tapering with tapered angle $\psi < 0$ and non-tapered artery with tapered angle $\psi = 0$. What's more, with an increase in $\mathrm{G_r}$, $\mathrm{G_c}$, the wall shear stress decrease a lot, which means that temperature and concentration profile have a negative effect on wall shear stress.

6.4 Flow resistance

Figure 8 and Figure 9 reveal the flow resistance profile for different values of ψ, $\mathrm{G_r}$ and $\mathrm{G_c}$ with $z = 10, t = 0.2, \mathrm{Re} = 1000, \alpha^2 = 2000, \tau_0 = 1, l = 4, \mathrm{E_c} = 0.4, \mathrm{P_r} = 3, \mathrm{S_r} = 3, \mathrm{S_c} = 3$. It is obviously that blood flow resistance reaches the maximum value at the critical height point of the stenosis from Figure 8 and Figure 9. The shape of the resistance distribution is like the opposition of flow rate as in Figure 4. It can also be proved from Eq. (5.25) and Eq. (5.26). Moreover, With the increase of Grashof number $\mathrm{G_r}$ and solutal Grashof number $\mathrm{G_c}$, the flow resistance reduces and it will decreases as the angle of tapered vessel increases.

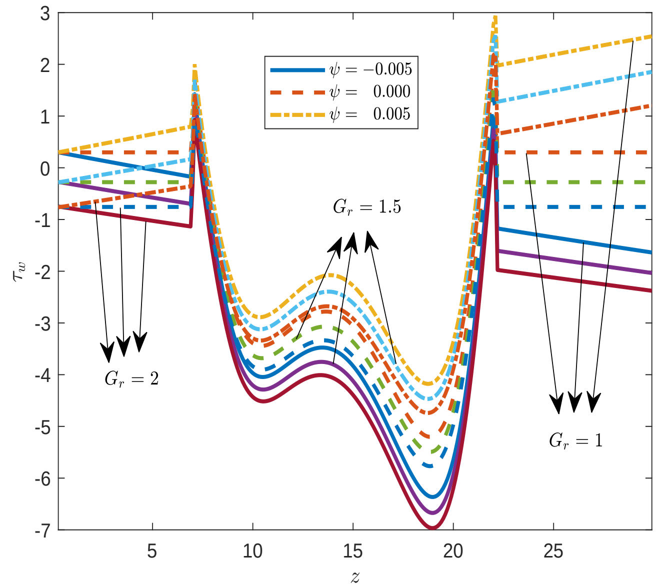

Figure 6: Variation of wall shear stress for $t = 0.2, \tau_m = 0.3d_0, \mathrm{Re} = 1000, \alpha^2 = 2000, \tau_0 = 1, l = 4, \mathrm{E_c} = 0.4, \mathrm{P_r} = 3, \mathrm{S_r} = 3, \mathrm{S_c} = 3, \mathrm{G_c} = 1.5$.

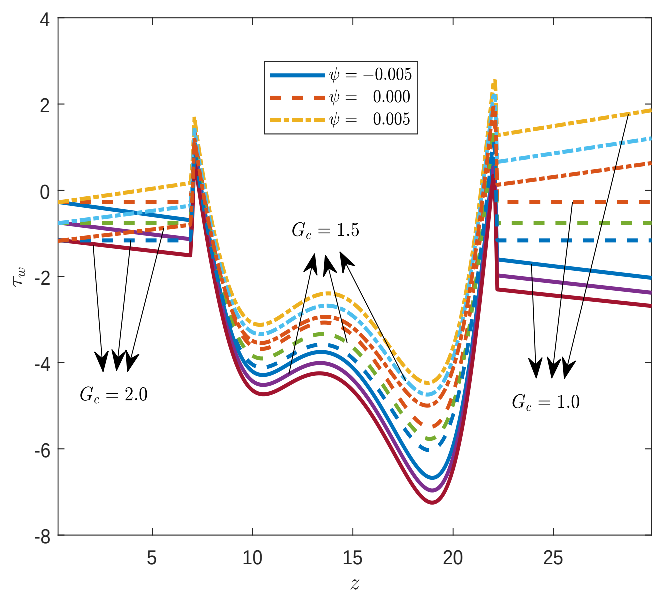

Figure 7: Variation of wall shear stress for $t = 0.2, \tau_m = 0.3d_0, \mathrm{Re} = 1000, \alpha^2 = 2000, \tau_0 = 1, l = 4, \mathrm{E_c} = 0.4, \mathrm{P_r} = 3, \mathrm{S_r} = 3, \mathrm{S_c} = 3, \mathrm{G_r} = 1.5$.

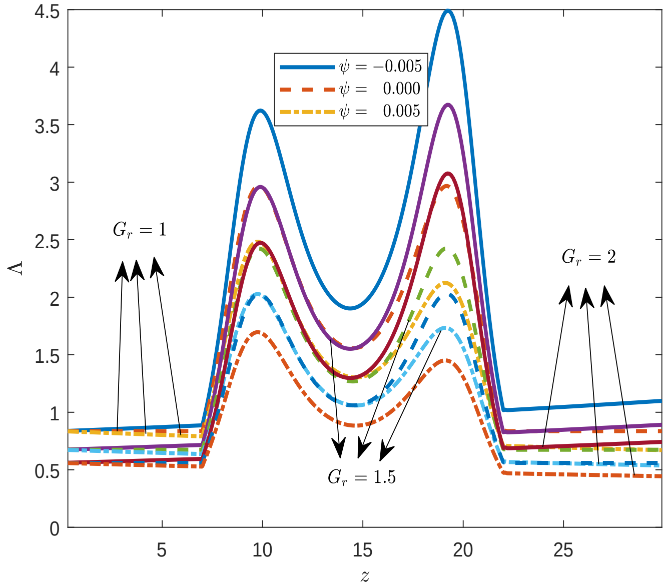

Figure 8: Variation of flow resistance for $t = 0.2, \tau_m = 0.3d_0, \mathrm{Re} = 1000, \alpha^2 = 2000, \tau_0 = 1, l = 4, \mathrm{E_c} = 0.4, \mathrm{P_r} = 3, \mathrm{S_r} = 3, \mathrm{S_c} = 3, \mathrm{G_c} = 1.5$.

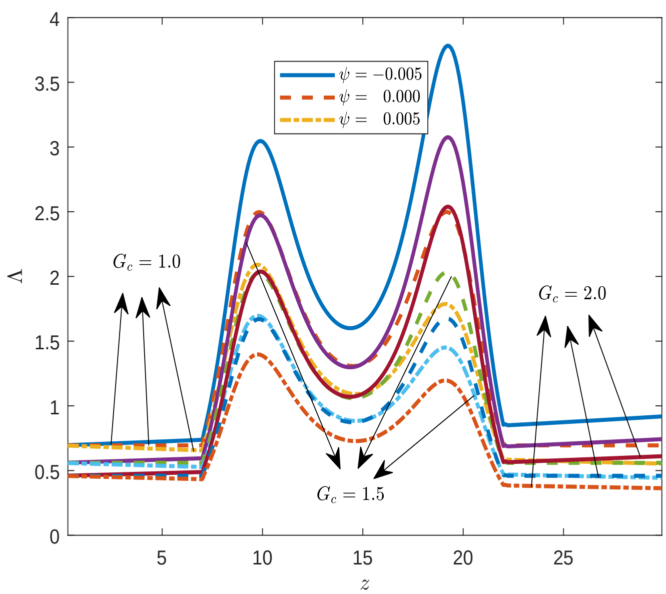

Figure 9: Variation of flow resistance for $t = 0.2, \tau_m = 0.3d_0, \mathrm{Re} = 1000, \alpha^2 = 2000, \tau_0 = 1, l = 4, \mathrm{E_c} = 0.4, \mathrm{P_r} = 3, \mathrm{S_r} = 3, \mathrm{S_c} = 3, \mathrm{G_r} = 1.5$.

7 Conclusion

The present mathematical analysis propounds several useful fluid dynamical properties of blood when it flows through tapered narrow arteries with mild overlapping time-dependent stenosis under heat and mass transfer. It reveals that the axial velocity of blood, flow rate, wall shear stress and resistance to flow are greatly influenced by blood rheology wall movement presence of stenosis, degree of taperness of the artery, heat transfer and mass transfer. The major results of the present investigation are:

- With the increase of maximum depth of the stenosis τ_m, the axial velocity of blood decreases while it will also decrease as the angle of tapered vessel increases.
- With the growth of Grashof number $\mathrm{G_r}$ and solutal Grashof number $\mathrm{G_c}$, the flow rate will increase a lot correspondingly, which means the positive feedback of heat and mass transfer on the velocity profile of blood.
- The wall shear stress distribution shaped like the distribution of flow rate and have similar response from different tapered angle and Grashof number $\mathrm{G_r}$ and solutal Grashof number $\mathrm{G_c}$
- It is observed that the resistive impedance in a diverging tapering appear to be smaller than those in a converging tapering because the flow rate is higher in the former than in the latter, as anticipated.
- It is seen that the flow resistance decrease when the Grashof number and solutal Grashof number increases, which means the negative feedback of heat and mass transfer on the blood resistance.

The study gives a further motivation to incorporate more realistic constitutive equations in the present model to represent the blood rheology and provides some quantitative guidance in clinical analysis.

Acknowledgments

This work was supported by the National Natural Science Foundation of China [grant number 11771216], the Natural Science Foundation of Jiangsu Province [grant number BK20151523], the Six Talent Peaks Project in Jiangsu Province [grant number 2015-XCL-020] and the Qing Lan Project of Jiangsu Province.

References

[1] N. S. Akbar, Biomathematical study of Sutterby fluid model for blood flow in stenosed arteries, Int. J. Biomath. **8** (2015) no. 6, 1550075–1–12.

[2] N. S. Akbar, Blood flow suspension in tapered stenosed arteries for Walter's B fluid model, Comput. Meth. Prog. Bio. **132** (2016), 45–55.

[3] N. S. Akbar and S. Nadeem, Carreau fluid model for blood flow through a tapered artery with a stenosis, Ain Shams Eng. J. **5** (2014), no. 4, 1307–1316.

[4] N. S. Akbar et al., Blood flow study of Williamson fluid through stenosed arteries with permeable walls, Eur. Phys. J. Plus **129** (2014), no. 11, 256.

[5] N. Ali, A. Zaman and M. Sajid, Unsteady blood flow through a tapered stenotic artery using Sisko model, Computers & Fluids **101** (2014), 42–49.

[6] E. H. Bloch, A quantitative study of the hemodynamics in the living microvascular system, Am. J. Anat. **110** (1962), no. 2, 125–153.

[7] S. Chakravarty and P. K. Mandal, A nonlinear two-dimensional model of blood flow in an overlapping arterial stenosis subjected to body acceleration, Math. Comput. Model. **24** (1996), no. 1, 43–58.

[8] P. Chaturani and R. P. Samy, Pulsatile flow of Casson's fluid through stenosed arteries with applications to blood flow, Biorheology **23** (1986), no. 5, 499–511.

[9] A. P. Dwivedi, T. S. Pal and L. Rakesh, Micropolar fluid model for blood flow through small tapered tube, Indian J. Technology **20** (1982), no. 8, 295–299.

[10] R. Ellahi, S. U. Rahman and S. Nadeem, Blood flow of Jeffrey fluid in a catherized tapered artery with the suspension of nanoparticles, Physics Letters A **378** (2014), no. 40, 2973–2980.

[11] A. R. Haghighi and M. S. Asl, Mathematical modeling of micropolar fluid flow through an overlapping arterial stenosis, Int. J. Biomath. **8** (2015), no. 4, 1550056–1–15.

[12] D. N. Ku, Blood flow in arteries, Annu. Rev. Fluid Mech. **29** (1997), no. 1, 399–433.

[13] S. Kumar and D. Kumar, Research note: oscillatory MHD flow of blood through an artery with mild stenosis. IJE. Trans. A Basics **22** (2009), no. 2, 125–130.

[14] X. Y. Luo, and Z. B. Kuang, A study on the constitutive equation of blood, J. Biomech. **25** (1992), no. 8, 929–934.

[15] P. K. Mandal et al., Effect of body acceleration on unsteady pulsatile flow of non-Newtonian fluid through a stenosed artery, Appl. Math. Comput. **189** (2007), no. 1, 766–779. MR2330254.

[16] K. S. Mekheimer and M. A. El Kot, Mathematical modelling of unsteady flow of a Sisko fluid through an anisotropically tapered elastic arteries with time-variant overlapping stenosis, Appl. Math. model. **36** (2012), no. 11, 5393–5407.

[17] E. W. Merrill et al., Pressure flow relations of human blood in hallow fibers at low shear rates, J. Appl. Physiol. **20** (1965), no. 5, 954–967.

[18] S. Nadeem et al., Power law fluid model for blood flow through a tapered artery with a stenosis, Appl. Math. Comput. **217** (2011), no. 17, 7108–7116.

[19] S. Priyadharshini and R. Ponalagusamy, Mathematical modelling for pulsatile flow of Casson fluid along with magnetic nanoparticles in a stenosed artery under external magnetic field and body acceleration, Neural Comput. Appl. (2017), 1–14.

[20] D. S. Sankar and U. Lee, FDM analysis for MHD flow of a non-Newtonian fluid for blood flow in stenosed arteries, J. Mech. Sci. Technol. **25** (2011), no. 10, 2573.

[21] M. K. Sharma, K. Bansal and S. Bansal, Pulsatile unsteady flow of blood through porous medium in a stenotic artery under the influence of transverse magnetic field, Korea-Aust. Rheol. J. **24** (2012), no. 3, 181–189.

[22] S. Shaw, P. V. S. Murthy and S. C. Pradhan, The effect of body acceleration on two dimensional flow of Casson fluid through an artery with asymmetric stenosis, The Open Conservation Biology Journal **2** (2010), no. 1.

[23] G. B. Thurston, Viscoelastic properties of blood on analoges, Advances in Hemodynamics and hemorheology **1** (1996), 1–30.

[24] D. Tripathi et al., Electro-magneto-hydrodynamic peristaltic pumping of couple stress biofluids through a complex wavy micro-channel, J. Mol. Liq. **236** (2017), 358–367.

[25] C. Tu and M. Deville, Pulsatile flow of non-Newtonian fluids through arterial stenosis, J. Biomech. **29** (1996), no. 7, 899–908.

[26] M. Waqas et al., Cattaneo-Christov heat flux model for flow of variable thermal conductivity generalized Burgers fluid, J. Mol. Liq. **220** (2016), 642–648.

[27] D. F. Young, Effects of a time-dependent stenosis on flow through a tube, J. Eng. Ind. **90** (1968), no. 2, 248–254.

[28] D. F. Young, Fluid mechanics of arterial stenosis, J. Eng. Ind. **101** (1979), no. 3, 157–175.

[29] A. Zaman et al., Effects of unsteadiness and non-Newtonian rheology on blood flow through a tapered time-variant stenotic artery, AIP advances **5** (2015), no. 3, 037129–1–13.